Utility of cone-beam computed tomography in the assessment of the porto-spleno-mesenteric venous system

Karunakaravel Karuppasamy

Cardiovascular and Interventional Radiology, Cleveland Clinic, Cleveland, USA

Correspondence to: Karunakaravel Karuppasamy. Cardiovascular and Interventional Radiology, Cleveland Clinic, Cleveland, USA. Email: karuppk@ccf.org.

Abstract: The common diagnostic tools available to evaluate the porto-spleno-mesenteric venous (PSMV) system provide either good hemodynamic information with limited morphological details [e.g., ultrasonography (US)] or excellent tomographic display of the anatomy with limited information about flow patterns [e.g., multidetector computed tomography (MDCT) and magnetic resonance imaging]. Although catheter-directed selective digital subtraction angiography (DSA) can provide excellent information about flow at a high temporal resolution and can generate images at a high spatial resolution, this technique is often limited by a lack of cross-sectional detail. In the assessment of the PSMV system, DSA is also limited by dilution of contrast and motion artefacts. Combining venous phase cone-beam computed tomography (CBCT) with DSA can generate high-quality tomographic data, which allows detailed evaluation of venous tributaries and flow patterns within the splenic, superior mesenteric, and inferior mesenteric venous systems individually. This enables clinicians to better understand the impact of nonobstructive resistance to flow (e.g., as in patients with cirrhosis) and obstructive resistance to flow (e.g., as in patients with thrombosis) within each system and plan treatment accordingly. In this review, we discuss the limitations of common diagnostic methods and the role venous CBCT in combination with DSA can play in assessing the PSMV system.

Keywords: Cone-beam computed tomography (CBCT); porto-spleno-mesenteric venous (PSMV); varices; portomesenteric thrombosis; portal hypertension

Introduction

The porto-spleno-mesenteric venous (PSMV) system is composed of the splenic vein (SpV), superior mesenteric vein (SMV), inferior mesenteric vein (IMV), and portal veins and their tributaries. The SMV and IMV serve as major outflows of blood from the small and large bowel, respectively. The SpV carries blood from the spleen, most of the pancreas, and part of the stomach. The mesenteric veins and SpV unify to form the main portal vein (MPV), which carries blood to the liver. Parts of the esophagus, stomach, and pancreas drain directly into the MPV.

Various disease processes affect the PSMV system, ranging from primary disease in the vessels resulting in flow impedance and secondary impedance in otherwise normal vessels due to resistance from portal hypertension.

This article reviews the anatomy and hemodynamics of the PSMV system and the various imaging modalities available to assess this system, with a special emphasis on cone-beam computed tomography (CBCT).

Normal and variant PSMV anatomy

Understanding the anatomy of the PSMV system in both healthy and diseased states is important in planning and performing procedures (1). In standard portal vein anatomy, the MPV divides into the left and right portal veins; the right portal vein subsequently divides into the right anterior portal vein, which supplies segments V and VIII, and the right posterior portal vein, which supplies segments VI and VII. However, standard anatomy is seen in only 65% of patients. Trifurcation is seen in 9%, and

other variants account for the rest (2). Variations in the SMV and IMV have also been reported. In one study, SMV was found to be a single trunk of variable length in 85% of patients; the remaining patients had two mesenteric trunks merging separately with the SpV (3). In the same study, the IMV was found to drain into the SpV in most patients; however, in one-quarter of patients, it drained into the SMV, and in nearly one-fifth of patients, it drained into the splenomesenteric angle. Such variations can also occur in the tributaries of these veins. One study demonstrated that the middle colic vein drained into the SMV in 63% of patients, into the gastrocolic trunk in 29%, into the IMV in 5%, into the SpV in 3%, and into the jejunal vein in 0.6% (4).

Hemodynamics and streamlining in the PSMV system

In the early development of the vascular system, hemodynamic stress is important for the differentiation of stem cells into vascular endothelial cells (5). When there is complete congenital systemic shunting of the splenomesenteric venous blood, intrahepatic portal veins fail to develop (6). After normal development, for maintenance of hepatic structure and function, hepatotrophic factors that originate from the pancreas need to be carried to the liver (7). The hepatocytes within the lobe that receives venous blood from the pancreas, stomach, and duodenum are large; those within the lobe that receives intestinal blood are small (7). In cirrhosis, changes to hemodynamic forces and preferential streaming of hepatotrophic factors are believed to play a key role in regional changes in hepatic morphology, such as hypertrophy of the caudate lobe and atrophy of the right lobe (8,9), and the same forces influence the development of collaterals (10).

Normal blood flow from the SMV, IMV, and SpV is often not equally distributed in the liver. In healthy individuals, in spite of confluence of these veins, the flow within the MPV is streamlined (i.e., appears to maintain a line of flow within the MPV with less turbulence or admixture). In normal individuals, blood flow from the SMV and IMV drain frequently distributes preferably into the right lobe or equally into both lobes, and not into left lobe (11). Further streamlining with these veins likely explains the preferential spread of disease in the liver. For instance, 90% of solitary liver abscesses (12) and 70% of hydatid liver cysts (13) occur in the right lobe. Right-sided colon cancers often metastasize to the right lobe, whereas left-sided tumors involve the entire liver (14). Any resistance to hepatopetal flow can affect this streamlining. In cases of cirrhosis, the SMV flow is left lobe predominant in 24% of patients, and in most patients, IMV flow cannot be seen in the liver (11).

Flow resistance and collateralization in the PSMV system

In healthy patients, the direction of blood flow in the PSMV system is consistently hepatopetal. Increased resistance to this flow can be seen in nonobstructive parenchymal disease such as cirrhosis or vascular obstructive disease such as thrombosis. Upstream resistance and subsequent back pressure result in engorgement of downstream tributaries initially outside the gut wall (e.g., paraesophageal), followed by dilatation of veins on the wall (e.g., periesophageal) and finally within the wall (e.g., submucosal and subepithelial). As the resistance increases, there is redirection of blood flow. Collateralization aims to return blood to the liver via porto-portal collaterals or into systemic circulation via porto-systemic collaterals or both (15). There are a few common and several uncommon sites for these collaterals (16). In cases of intrahepatic resistance, the flow is hepatofugal via portosystemic collaterals. When the obstruction is extrahepatic, there is often a combination of portosystemic and porto-portal collaterals occurring in the hepatofugal and hepatopetal directions, respectively. When there is resistance to the normal flow of blood, the clinical presentation and formation of collaterals vary depending on the underlying cause and the downstream territory affected by the back pressure (17,18).

Imaging techniques to assess PSMV system

Several imaging methods are available to study the PSMV system (*Table 1*). Some of these methods provide extensive morphological information but limited detail regarding flow dynamics, whereas others provide excellent information regarding flow dynamics but limited morphological information.

Transabdominal ultrasonography (US) is inexpensive, readily available, portable, and well tolerated. The sensitivity and specificity of detecting a thrombus of the MPV are high and are further improved when color Doppler techniques are used (19). However, this method is technically demanding, and both operator dependency and interobserver variability are high (20). In addition, in

Table 1 Imaging techniques to assess the PSMV system

Noninvasive methods
Transabdominal US
MDCTA
MRA
Less invasive methods
Endoscopic US
Transarterial indirect venography
DSA alone
DSA and venous phase CBCT
More invasive methods
Percutaneous transhepatic direct portal venography*
DSA alone
DSA and venous phase CBCT
Transjugular intrahepatic direct portal venography*
DSA alone
DSA and venous phase CBCT
Direct splenic venography*
DSA alone
DSA and venous phase CBCT

*, does not demonstrate upstream venous tributaries. PSMV, porto-spleno-mesenteric venous; US, ultrasonography; MDCTA, multidetector computed tomography angiography; MRA, MR angiography; DSA, digital subtraction angiography; CBCT, cone-beam computed tomography.

acutely ill patients, transabdominal US can be a prodigious undertaking (21). Finally, assessment with this technique is often limited to major intrahepatic and extrahepatic veins; assessment of flow within smaller distant tributaries is not possible.

Endoscopic US (EUS) performed at various points in the stomach and duodenum can effectively assess central PSMV veins. EUS also provides higher-resolution images and can more consistently evaluate the supraduodenal, infraduodenal, and retroduodenal segments of the portal vein and SpV as well as the major tributaries of these veins near the portal vein confluence. However, EUS is invasive, is heavily user dependent, and often cannot demonstrate the entire course of vessels (22).

Contrast-enhanced multidetector computed tomography

(MDCT) can evaluate the entire PSMV system, is not heavily operator dependent, and is unaffected by bowel gas. MDCT is widely available, completed within a few minutes, and well tolerated by patients. MDCT angiography (MDCTA) is widely used for evaluating arterial and venous disease in the splanchnic circulation. MDCTA has excellent sensitivity and specificity (19). Although MDCT has demonstrated a positive correlation between the size of the SMV and right hepatic lobe and between the SpV and both lobes of the liver (23), direct information on flow such as velocity, pressure, and direction cannot be obtained with this technique.

Gadolinium-enhanced MR angiography (GE-MRA) offers a good alternative to iodinated contrast-based MDCTA, and at a high spatial resolution, it provides a detailed overview of the PSMV system. MRA can also identify the varices/collaterals in cases of chronic occlusion and bowel wall edema in cases of acute occlusion. A variant of GE-MRA, four-dimensional (4D) time-resolved MRA, can demonstrate flow patterns within complex vascular anatomy, albeit at a lower spatial resolution. When allergies or severe renal dysfunction preclude the administration of contrast material, noncontrast MRA sequences such as Time-of-Flight (ToF) MRA and phase-contrast (PC) MRA can provide useful information, including information about direction and velocity, respectively (24). Newer 4D flow-sensitive noncontrast MRA techniques can be used to qualitatively and quantitatively study blood flow (25). However, there is a significant discrepancy between these techniques and Doppler US for several indices used to quantity flow (26), and so these methods are not widely used in the clinical setting. In spite of the major advantage of lack of exposure to ionizing radiation, MRA of PSMV system is remains as a useful option only in special circumstances due to a several reasons—high cost, limited availability, longer scan times compared to MDCT, artifacts, and contraindications of MRI (19).

Dedicated interventional suites with built-in C-arm fluoroscopic systems are widely available and used to study vascular anatomy using digital subtraction angiography (DSA). With this technique, a contrast agent is injected into the blood vessels and multiple two-dimensional (2D) images are generated at high temporal resolution and excellent in-plane spatial resolution. This technique can be used to analyze vascular lumen and evaluate the flow of blood. This is often considered a gold-standard technique, although it is invasive.

DSA of the PSMV system can be performed directly

Table 2 Strengths of venous CBCT plus DSA versus MDCT and DSA alone in assessment of the PSMV system

Features	MDCT	DSA	DSA + venous CBCT
Luminal thrombus	+++	+	+++
Stenosis/occlusions	+++	++	+++
Large veins	+++	++	+++
Small veins	+	+	+++
Major collaterals	+++	+++	+++
Minor collaterals	++	+	+++
Flow dynamics*	+	++	+++

*, ability to accurately locate flow and identify flow direction; +, represents assessment to be suboptimal; ++, is satisfactory; +++, is optimal. CBCT, cone-beam computed tomography; DSA, digital subtraction angiography; MDCT, multidetector computed tomography; PSMV, porto-spleno-mesenteric venous.

or indirectly. In the direct method, access is obtained directly into the portal vein via a percutaneous transhepatic or transjugular intrahepatic approach or into a SpV via a percutaneous transplenic approach, and contrast medium is injected. This technique is more invasive and does not allow evaluation of upstream tributaries; therefore, it is reserved for direct delivery of therapy such as embolization and angioplasty (19). In the indirect method, each of the PSMV tributaries is studied independently by selectively injecting contrast material using a catheter into the inflow artery, often inserted via common femoral artery. The indirect method is less invasive and is the DSA method of choice (19).

Evaluation of small tributaries within the PSMV system is often suboptimal; this is due to a combination of factors. There is significant dilution of contrast material when the contrast bolus reaches the larger pool of venous blood, and the subtraction artifacts caused by breathing and peristalsis are more pronounced during the later phases of DSA. Another limitation of 2D DSA is its inability to accurately assess overlapping loops of vessels.

Assessment of the PSMV system could be improved if one could visualize vessels in three dimensions using the same equipment. To this end, CBCT can be combined with DSA to evaluate the PSMV system.

CBCT in interventional radiology

The C-arm systems now present in many interventional suites have a 2D flat panel detector and can perform CBCT and acquire a complete volumetric data set in a single gantry rotation. With improvements in hardware technology and reconstruction algorithms, these 2D flat panel detector-based systems can generate volumetric data at higher spatial resolution with improved low-contrast detectability and in multiplanar formats (27). This allows for a single system in the interventional radiology suite that is capable of generating both 2D images and 3D data, thus providing the benefits of both DSA and MDCTA in the same room (*Table 2*).

CBCT has proven its value within radiology. It is often used to evaluate small bones and joints (28), demonstrate complex vascular anatomy, diagnose intracranial bleed, evaluate the patency of stents, and assess the adequacy of coil packing (29). When used with DSA during transarterial chemoembolization, CBCT prolongs survival in patients with unresectable hepatocellular carcinoma (30). During selective internal radiation therapy, CBCT has higher sensitivity in identifying extrahepatic enhancement than DSA (31).

A single DSA examination generates a series of images that provide information on blood flow when contrast moves from one vascular territory to another during the course of image acquisition; these results are viewed in a single plane. On the other hand, a single CBCT scan provides 3D data for complex vascular territories, which can then be reformatted to be viewed in many planes. Although the use of CBCT timed to the arterial phases has been explored for many angiographic applications, the role of CBCT in evaluating the venous anatomy has not been adequately explored. We retrospectively evaluated venous CBCT in eight patients with known portomesenteric venous thrombosis. CBCT provided higher quality images of venous drainage pathways than DSA and identified a greater number of minor and portoportal collateral pathways than DSA (32). While MDCTA and DSA are both useful in the evaluation of PSMV, they are performed on two different radiographic systems. CBCT performed using the same equipment as DSA can harness the individual advantages of MDCTA and DSA (*Table 2*).

Technical aspects of CBCT for evaluation of the PSMV system

Whereas state-of-the-art 64-slice MDCT can generate information from an isotropic voxel size of $600 \times 600 \times 600 \ \mu m^3$, isotropic voxel sizes of less than $200 \times 200 \times 200 \ \mu m^3$ are theoretically achievable with current C-arm
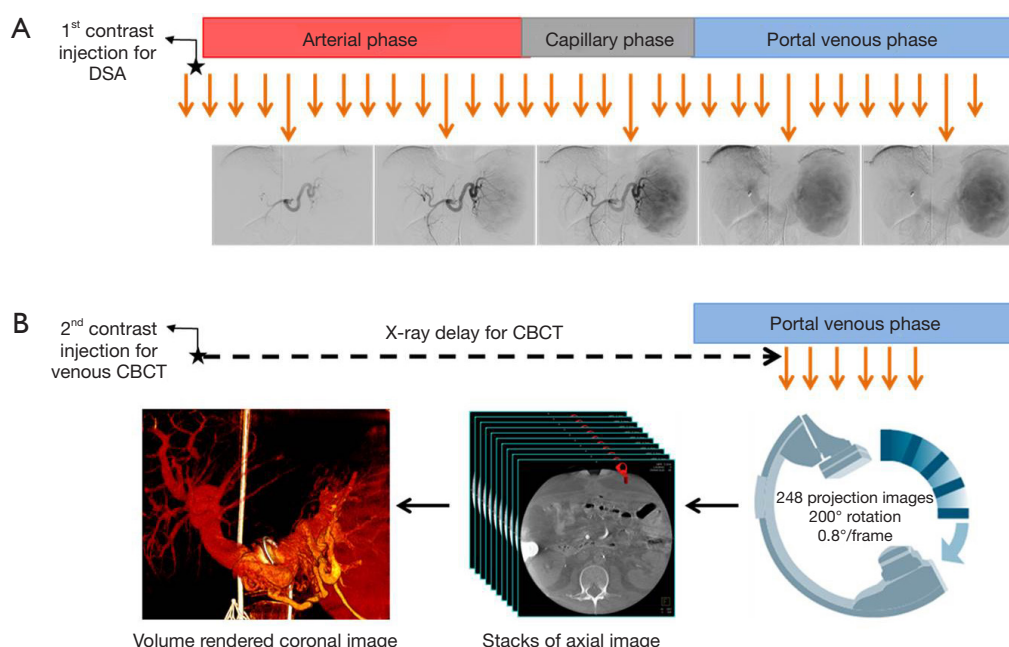
Figure 1 Guide to venous CBCT. (A) After the first contrast injection, DSA is obtained. Venous phases are closely reviewed, and the time taken for ideal PSMV opacification from the start of contrast injection is calculated; (B) after the second contrast injection, once the calculated delay has passed, CBCT is triggered. CBCT, cone-beam computed tomography; DSA, digital subtraction angiography; PSMV, porto-spleno-mesenteric venous.

CBCT systems using a flat-panel detector. However, blur caused by the X-ray converter and reconstruction filter, protracted reconstruction times, and radiation dose considerations often prevent the achievement of such high spatial resolution (27). In addition, CBCT has increased scattered radiation and significant noise and image quality degradation versus MDCT, likely because of differences in geometry (cone-beam *vs.* fan-beam) and the presence of antiscatter septae between the individual detector channels in MDCT (27). To achieve high-quality images on CBCT, the operator may have to increase the dose, the slice thickness, or both (33). When clinical protocols are used with acceptable levels of noise, the spatial resolution of CBCT is comparable to that of MDCT for high-contrast anatomy. However, for low-contrast structures, the spatial resolution of CBCT remains inferior (34).

To assess the PSMV system with CBCT, the operator must ensure that adequate high-density contrast reaches the veins. To this end, CBCT should be timed to acquire the projectional images necessary for reconstruction only after all of the major veins and their tributaries have been fully opacified and remain opacified when the gantry rotates. There is a delay between the initiation of contrast injection

into a major splanchnic artery and the opacification of the veins in that territory. In the splenic territory, this delay is short compared to the delay in the superior mesenteric vascular bed. When there is obstruction to venous outflow, the delay is longer, and the contrast sometimes takes one of many tortuous routes (16). Hence, this delay cannot be arbitrary and is not always predictable. In our practice, we always measure this delay using DSA (*Figure 1*). DSA images after injection of the first dose of contrast material are reviewed for reflux of any contrast, adequacy of contrast injection, and appearance of the venous anatomy. Based on this, the parameters for injection of the second dose of contrast material required for CBCT are adjusted and CBCT is triggered after the measured delay. Our general principles for DSA that are later adjusted for CBCT are as follows:

❖ The catheter should provide stability during contrast injection. The suggested choices of catheters and catheter tip locations are as follows.
   ◆ A 5F C2 catheter is advanced into the mid splenic artery;
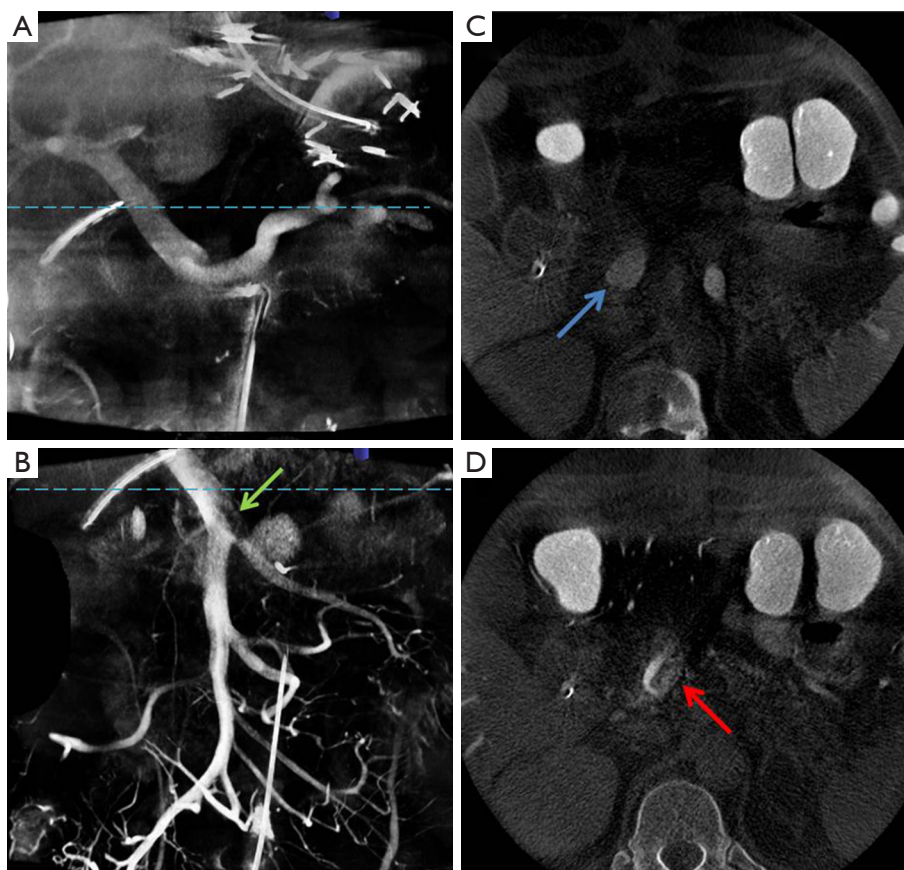   ◆ A 5F Sos catheter is advanced into the proximal superior mesenteric artery;

Figure 2 CBCT demonstrates venous tributaries and streamlined drainage in each of the PSMV territories individually. The dotted lines in (A) and (B) refer to the position of the axial images from (C) and (D), respectively. (A) Coronal SpV CBCT image demonstrates the SpV draining into the main, left, and right portal veins; (C) axial SpV CBCT image demonstrates near uniform opacification within the MPV (blue arrow); (B) coronal SMV CBCT image demonstrates the SMV draining into the MPV with streamlining artefact at the splenomesenteric confluence (green arrow); (D) axial SMV CBCT image demonstrates streamlining artefact within the MPV (red arrow). CBCT, cone-beam computed tomography; PSMV, porto-spleno-mesenteric venous; SpV, splenic vein; MPV, main portal vein; SMV, superior mesenteric vein.

- A microcatheter is advanced via a 5F Sos catheter into the proximal inferior mesenteric artery.
❖ Dilution of the contrast agent is expected as the contrast bolus reaches the PSMV system.
  - An undiluted full-strength contrast agent with high iodine content (e.g., 350 mgI/mL) is preferred.
❖ Adequate volume of contrast material should be injected at an appropriate rate. The suggested injection volumes and rates are as follows.
  - About 24 to 30 cc at 4 to 5 cc/s into the splenic artery;
  - About 30 to 40 cc at 5 to 6 cc/s into the superior mesenteric artery;
  - About 9 to 12 cc at 1.5 to 2 cc/s into the inferior mesenteric artery.

CBCT evaluation of individual drainage systems

The PSMV system consists of three independent drainage systems, and assessment of each drainage system requires isolated visualization of the veins within that system. With MDCTA or GE-MRA, the entire PSMV territory is opacified simultaneously and assessment of individual systems is limited. Identifying flow in the venous tributaries within each drainage system would require selective injection of contrast into the feeding arteries. DSA generates 2D images of the veins in each system in a single plane, whereas CBCT demonstrates the same anatomy in great detail in multiple reconstructed planes (*Figure 2*). Unlike MDCTA, where streamlined artifacts are not seen, these artifacts may appear on CBCT

because of opacified blood from one territory mixing with unopacified blood flowing from another. The presence of these artifacts depends on the level of mixing that occurs at these confluences. SpV blood flow is seen to uniformly opacify the MPV, which is in line with studies suggesting equal distribution of SpV blood between the right and left lobes. However, SMV flow is streamlined within the MPV in keeping with its preferential flow into the right lobe in many patients (*Figure 2A*) (11,23,35).

Tomographic advantage of CBCT

Because of the large capacitance of the venous system, the shape of the venous wall varies greatly depending on pressure, volume, and flow. When pressure is low, the veins are easily collapsible and elliptical in shape. With small increases in pressure, the vessel compensates by distending and taking on a more rounded shape (36,37). Thus, change in size of veins does not always equate to the hemodynamic pressure gradient. One study found that a peak vein velocity ratio of >2.5 across a stenosis better correlated with a pressure gradient of 3 mmHg (38), and research has shown that there is a correlation between increasing degree of collateral pathways and stenosis scores (39). MDCTA and GE-MRA can be used to assess the size of veins and to visualize the collaterals. However, the back pressure caused by a stenosis cannot be measured and the pressure may not affect all downstream territories equally, and so collateral formation is likely to be different within each downstream territory. Venous CBCT combined with DSA can assess a stenosis in cross section, visualize flow across/around it via collaterals, and thus clearly demarcate the downstream impact it has within each territory.

The tomographic advantage of CBCT was demonstrated in the case of a patient who was referred to our institution 7 weeks after receiving isolated small bowel transplant. Routine follow-up MDCTA demonstrated near-occlusive thrombosis within the interposition graft between the recipient and donor SMVs. However, a small bowel biopsy demonstrated no dilated veins to indicate back pressure, and MDCTA failed to identify any large collateral pathways. The transplanted superior mesenteric artery was accessed and DSA demonstrated several small collaterals with some draining into the portal vein; the final drainage of other collaterals could not be ascertained (*Figure 3A*). Venous CBCT angiography identified the presence, extent, and course of several collaterals. CBCT combined with DSA also confirmed the final drainage patterns; flow was hepatopetal

into the liver (portoportal collaterals) (*Figure 3B*) and hepatofugal into the systemic veins (portosystemic collaterals) (*Figure 3C*). This confirmed the adequacy of venous outflow from the transplanted small bowel, and no further interventions were considered necessary.

CBCT assessment of small veins

Typically, significant involvement of the portal vein, SpV, or SMV is a contraindication for surgical management of several types of intra-abdominal tumors. Arterial assessment with MDCTA is often of high quality because the actual arrival of contrast in the arterial tree is either measured ahead using a timing bolus technique or monitored live using a bolus tracking technique. However, arrival of contrast in mesenteric veins is not always predictable; hence, an arbitrary delay is used (50–100 s after the start of injection) to trigger venous phase MDCTA (40,41). Arterial phase MDCTA clearly demonstrates small arterial branches without any opacification of small veins. However, the assessment of small venous tributaries and their relationship with the tumor is limited because of contrast dilution and persistent opacification of adjoining arterial branches. In such cases, CBCT can demonstrate isolated venous anatomy by acquiring data when the contrast bolus has left the arterial tree and is in the veins.

The usefulness of CBCT was demonstrated in the case of a 71-year-old man with a partially calcified large confluent mesenteric mass treated at our institution. Surgical resection was planned; however, the extent of resection of small venous tributaries and small bowel that would be required to remove the mass could not be ascertained on MDCT. CBCT timed to the SMV phase was performed. Axial images (*Figure 4A,B*) and images obtained with the volume rendering technique (*Figure 4C*) clearly demonstrated the intricate relationship between the tumor and several small ileal veins. However, the jejunal, right colic, and middle colic veins were not involved. Surgical resection would have required removal of the ileum, resulting in short gut syndrome. A laparoscopic biopsy was instead performed. Sclerosing mesenteritis was diagnosed, and the case was managed conservatively.

CBCT for planning interventions

Transjugular intrahepatic portosystemic shunt (TIPS) creation can be used to manage variceal bleeding and refractory ascites secondary to portal vein thrombosis (PVT). In patients with chronic PVT, attempts are made
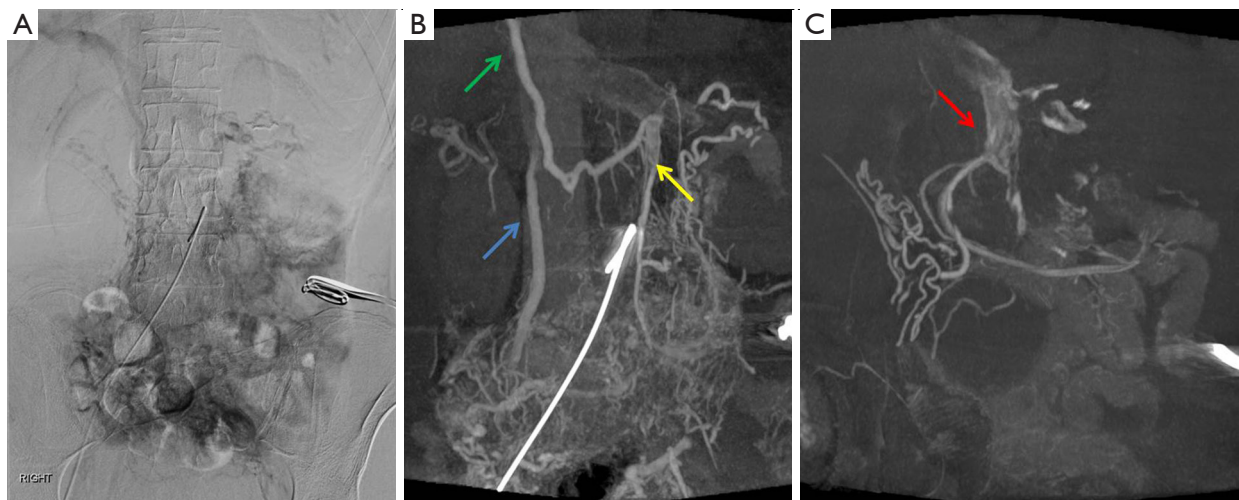
Figure 3 After receiving an isolated small bowel transplant 7 days earlier, a patient was incidentally found to have thrombosis of the interposition graft between the recipient and donor SMVs on MDCTA. To assess the adequacy of collateral formation, DSA was performed. (A) In a DSA image of the venous phase, assessment is limited because of overlapping loops of vessels, dilution of contrast, and subtraction artifacts; (B,C) coronal images from venous CBCT confirm occlusion at the venous anastomosis and several collateral pathways. There are two portoportal collateral pathways: one via the gastroepiploic vein (green arrow) and one into the stump of the native SMV (red arrow). There are three portosystemic collateral pathways: one via the right gonadal vein into the inferior vena cava (blue arrow), one via the left gonadal vein into the left renal vein (yellow arrow), and one via the left lumbar veins into the left common iliac vein (not shown). SMV, superior mesenteric vein; MDCTA, multidetector computed tomography angiography; DSA, digital subtraction angiography; CBCT, cone-beam computed tomography.
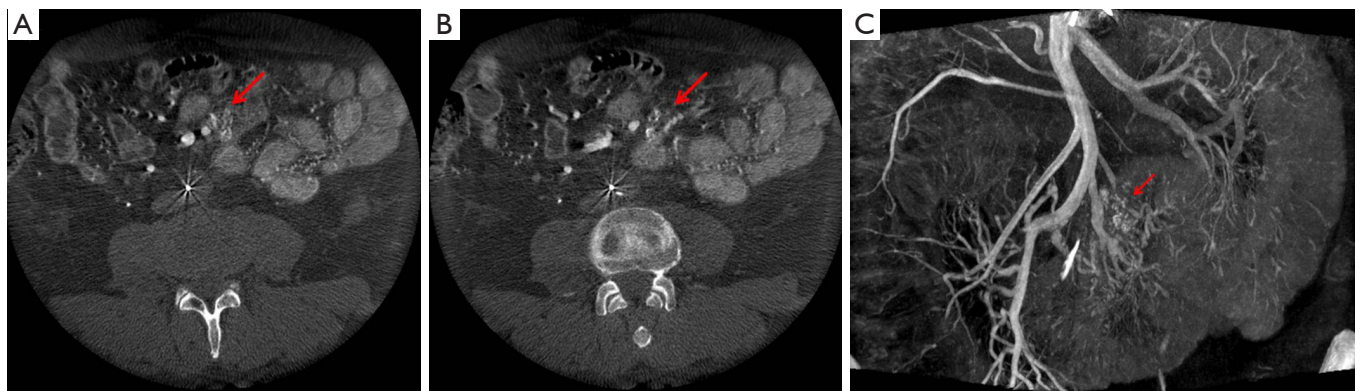

Figure 4 Surgical resection was planned for a patient with a partially calcified large confluent mesenteric mass. CBCT timed to the SMV phase was performed for evaluation. (A,B) Axial images clearly demonstrate the intricate relationship between the calcifications (red arrows) within the tumor and several small SMV tributaries; (C) a maximum intensity coronal reformed image demonstrates calcifications (red arrow) abutting ileal veins. Jejunal, right colic, and middle colic veins were not involved. CBCT, cone-beam computed tomography; SMV, superior mesenteric vein.
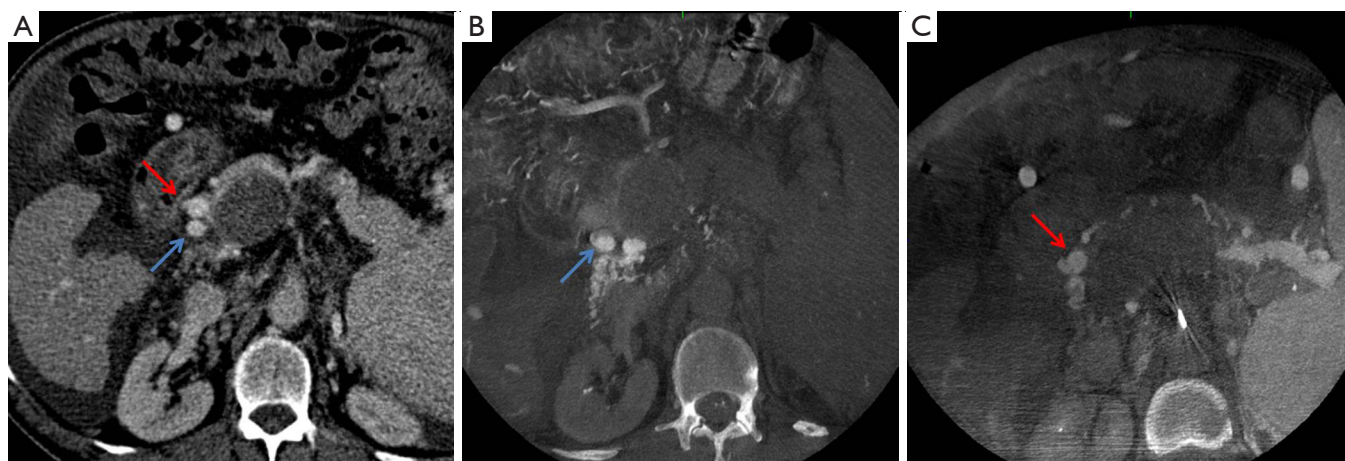
Figure 5 A patient with alcohol-induced cirrhosis complicated by refractory ascites and PVT extending into the SMV and SpV was evaluated for TIPS placement. (A) An axial MDCT image demonstrates two large periportal collateral veins (red and blue arrows); (B) an axial SMV CBCT image shows flow from the SMV tributaries only into the large periportal collateral vein along the right posterior wall of the thrombosed MPV (blue arrow); (C) an axial SpV CBCT image shows flow from the SpV tributaries predominantly into the large periportal collateral vein along the right anterior wall of the thrombosed MPV (red arrow). SMV, superior mesenteric vein; SpV, splenic vein; TIPS, transjugular intrahepatic portosystemic shunt; MDCT, multidetector computed tomography; CBCT, cone-beam computed tomography; MPV, main portal vein.

to recanalize the MPV via transjugular intrahepatic access. If this technique fails, the TIPS is placed between a hepatic vein and a large collateral vein (42). PVT can also extend into the SMV and/or SpV, which can result in variable pressures and collateralization in the downstream territories. Hence, when more than one collateral vein is present, the choice of collateral vein for TIPS placement is important (43). In extrahepatic PVT, ascites is more common when PVT involves the SMV than when it involves the SpV (44). In cases of isolated SpV thrombosis, ascites is uncommon; gastroesophageal variceal bleeding is the more serious complication (45). Identification of varices and flow pattern within the periportal collaterals is key to understanding the predominant vascular bed drained by each collateral. TIPS insertion into a collateral that primarily drains the SpV blood will likely decompress gastroesophageal varices, whereas TIPS insertion into a collateral that drains SMV blood will likely help to manage refractory ascites.

We treated a 64-year-old man with a history of alcohol-induced cirrhosis complicated by refractory ascites and PVT with extension into the SMV and SpV; the patient was awaiting liver transplant. To manage the ascites, we planned to create a TIPS. MDCTA identified two large periportal collateral veins (*Figure 5A*). However, the vascular bed

they drained could not be defined. We performed selective splenic and superior mesenteric angiograms; venous CBCT scans were also performed in each territory. SMV CBCT demonstrated a large periportal collateral vein along the right posterior wall of the thrombosed MPV, which drained predominantly into the right lobe (*Figure 5B*). SpV CBCT confirmed the presence of SpV occlusion and a large gastroepiploic vein draining into a large periportal collateral vein along the right anterior wall of the thrombosed MPV, which drained predominantly into the left lobe (*Figure 5C*). CBCT helped us to determine that the preferred target collateral vein to manage ascites in this patient was the one that drained the SMV bed; as such, a TIPS was created between the right hepatic vein and the large periportal collateral vein along the right posterior wall.

CBCT for intraprocedural guidance

CBCT can be used for guidance during procedures. A trajectory or soft tissue anatomy otherwise not visible on live fluoroscopic procedure can often be planned and identified with CBCT images. The trajectory can then be overlaid on the live image. Hawkins *et al.* (46) reported successfully using this technique to choose the target and skin entry sites for percutaneous nephrolithotripsy access in 12 nondilated
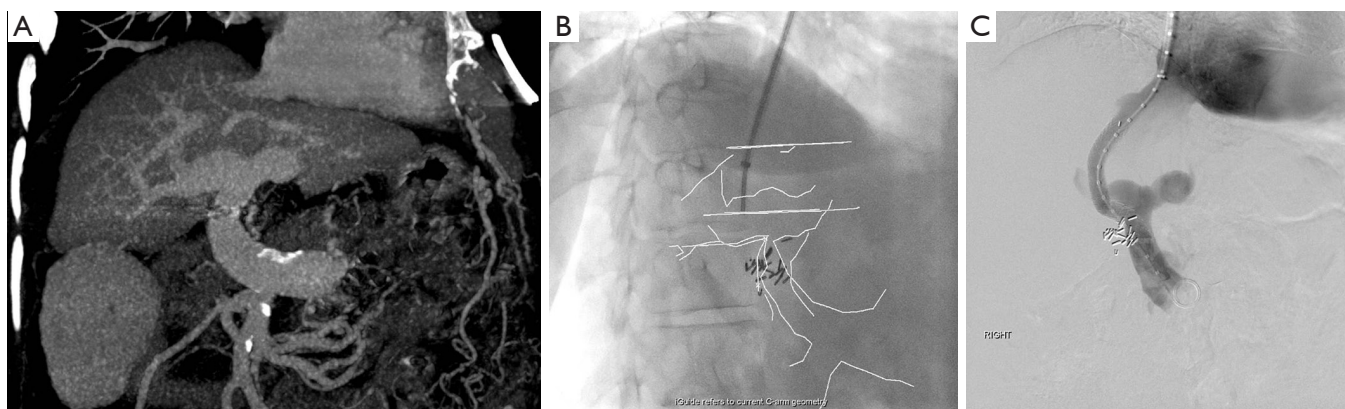
cdt.amegroups.com   *Cardiovasc Diagn Ther* 2016;6(6):544-556

Figure 6 A patient with nonalcoholic steatohepatitis and portal hypertension was referred for TIPS creation before resection of an invasive colorectal adenocarcinoma. (A) A coronal MDCT image showing the MPV and its bifurcation was obtained; (B) intraprocedural noncontrast CBCT was performed, and the outline from MDCT was registered with these results and displayed on a live fluoroscopy screen; (C) the portal vein was accessed, and TIPS was completed. TIPS, transjugular intrahepatic portosystemic shunt; MDCT, multidetector computed tomography; MPV, main portal vein; CBCT, cone-beam computed tomography.

collecting systems in nine patients. Alternatively, CBCT can be registered with another modality such as MDCT or MRI, and the fused data can be overlaid on live fluoroscopic images to enhance guidance (47).

At our institution, a 61-year-old woman with nonalcoholic steatohepatitis and portal hypertension presented with recurrent ascites and invasive adenocarcinoma. Liver transplant was deferred, and a colectomy with ileostomy was planned. TIPS creation was requested preoperatively to reduce the surgical risk for intraoperative bleeding and manage ascites postoperatively. During a typical TIPS procedure, before a needle is advanced from the hepatic vein into the portal vein, the anatomy of the portal veins is often evaluated using a reflux portogram with a catheter wedged into the liver parenchyma, which can sometimes fail to demonstrate the MPV. An alternative method was used in this patient: the contour of the MPV and its bifurcation was identified on preprocedural MDCTA (*Figure 6A*), and this was registered with intraprocedural noncontrast CBCT. This registration allowed the overlay of the contour on a live fluoroscopic screen (*Figure 6B*). The portal vein was then accessed and the TIPS procedure was completed (*Figure 6C*). Alternatively, an indirect DSA followed by venous phase CBCT can generate images of the PSMV using the same angiographic equipment, and the anatomy can be overlaid on a live screen without the need for registration. However, this method requires direct catheter access into the mesenteric or splenic artery. In a study by Ketelsen *et al*. (48), the usefulness of CBCT performed

after intravenous injection of contrast material to outline the portal vein was retrospectively compared with wedged reflux portogram; the study results confirmed a significantly lower procedural time with this method, which does not require registration with another modality or arterial access. However, 75 mL of contrast medium was used for CBCT. Thus, CBCT can be used in a number of ways for registration and guidance or guidance without the need for registration during procedures.

Current limitations of CBCT

Currently, 3D CBCT provides cross-sectional details of opacified anatomy at a single chosen phase of contrast enhancement. It lacks temporal resolution and cannot display actual flow of blood. Instead, DSA is used for that purpose. Time-resolved 4D CBCT can display actual flow of blood in cross section, especially in complex vascular pathways and perfusion within organs. However, 4D CBCT of the PSMV system at a high temporal resolution similar to that used for DSA would require a fast gantry rotation, which is not currently possible because of safety concerns (49). Within the current limitations, researchers successfully used 4D CBCT for endovascular stroke treatment on a biplane flat detector angiographic system using nine bidirectional rotational scans (50). With existing technology, 4D CBCT of the PSMV system at a lower temporal resolution is likely possible.

In current practice, CBCT always follows DSA,

necessitating an additional contrast dose. Because contrast volume is related to the risk of contrast-induced nephropathy (CIN) (51), the potential added value of CBCT should always be weighed against the risk of CIN. Estimated glomerular renal function is a useful predictor of CIN and can be used to adjust the volume of contrast agent administered (37). The risk of CIN can be reduced if the contrast volume is restricted to no more than 2.5 times the baseline estimated glomerular renal function (52).

Researchers using thermoluminescence dosimeters in head and body CT phantoms found that the added radiation dose with CBCT is not negligible when compared with MDCT (53). It is always important to follow the ALARA (as low as reasonably achievable) rule, preventing unnecessary radiation exposure by avoiding CBCT when not needed, optimizing the technical protocol, restricting the field of view, and shielding vital organs.

Conclusions

Venous phase CBCT can be a useful adjunct to DSA in assessing the PSMV anatomy. CBCT is especially useful in evaluating overlapping loops of collateral pathways in chronic occlusions. These 3D images can also be overlaid on live fluoroscopy to help guide procedures. However, users should be aware of the additional contrast volume and radiation involved in CBCT and should weigh these considerations against the potential benefit of CBCT.

Acknowledgements

Footnote

Conflicts of Interest: The author has no conflicts of interest to declare.

References

1. Erbay N, Raptopoulos V, Pomfret EA, et al. Living donor liver transplantation in adults: vascular variants important in surgical planning for donors and recipients. AJR Am J Roentgenol 2003;181:109-14.

2. Covey AM, Brody LA, Getrajdman GI, et al. Incidence, patterns, and clinical relevance of variant portal vein anatomy. AJR Am J Roentgenol 2004;183:1055-64.

3. Graf O, Boland GW, Kaufman JA, et al. Anatomic variants of mesenteric veins: depiction with helical CT venography. AJR Am J Roentgenol 1997;168:1209-13.

4. Maki Y, Mizutani M, Morimoto M, et al. The variations of the middle colic vein tributaries: depiction by three-dimensional CT angiography. Br J Radiol 2016;89:20150841.

5. Cartwright JH, Piro O, Tuval I. Fluid dynamics in developmental biology: moving fluids that shape ontogeny. HFSP J 2009;3:77-93.

6. Morgan G, Superina R. Congenital absence of the portal vein: two cases and a proposed classification system for portasystemic vascular anomalies. J Pediatr Surg 1994;29:1239-41.

7. Starzl TE, Francavilla A, Halgrimson CG, et al. The origin, hormonal nature, and action of hepatotrophic substances in portal venous blood. Surg Gynecol Obstet 1973;137:179-99.

8. Awaya H, Mitchell DG, Kamishima T, et al. Cirrhosis: modified caudate-right lobe ratio. Radiology 2002;224:769-74.

9. Tan KC. The right posterior hepatic notch sign. Radiology 2008;248:317-8.

10. Marks C. Developmental basis of the portal venous system. Am J Surg 1969;117:671-81.

11. Shiomi S, Kuroki T, Miyazawa Y, et al. Hepatic distribution of blood flow from the superior or inferior mesenteric vein mapped by portal scintigraphy with iodine-123-iodoamphetamine. J Nucl Med 1996;37:51-4.

12. Cuarón A, Gordon F. Liver scanning: analysis of 2,500 cases of amebic hepatic abscesses. J Nucl Med 1970;11:435-9.

13. Adams R, Hindawi AY, Qassab K. Localization of hydatid liver cysts with colloidal radiogold. International Atomic Energy Agency Scanning Program in Iraq. J Nucl Med 1962;3:315-22.

14. Shirai Y, Wakai T, Ohtani T, et al. Colorectal carcinoma metastases to the liver. Does primary tumor location affect its lobar distribution? Cancer 1996;77:2213-6.

15. Sharma M, Rameshbabu CS. Collateral pathways in portal hypertension. J Clin Exp Hepatol 2012;2:338-52.

16. Arora A, Rajesh S, Meenakshi YS, et al. Spectrum of hepatofugal collateral pathways in portal hypertension: an illustrated radiological review. Insights Imaging 2015;6:559-72.

17. Keiding S, Solvig J, Grønbaek H, et al. Combined liver vein and spleen pulp pressure measurements in patients with portal or splenic vein thrombosis. Scand J

Gastroenterol 2004;39:594-9.

18. Pereira P, Peixoto A. Left-sided portal hypertension: a clinical challenge. GE Port J Gastroenterol 2015;22:231-3.

19. Hauenstein K, Li Y. Radiological Diagnosis of Portal/Mesenteric Vein Occlusion. Viszeralmedizin 2014;30:382-7.

20. de Vries PJ, van Hattum J, Hoekstra JB, et al. Duplex Doppler measurements of portal venous flow in normal subjects. Inter- and intra-observer variability. J Hepatol 1991;13:358-63.

21. Parvey HR, Eisenberg RL, Giyanani V, et al. Duplex sonography of the portal venous system: pitfalls and limitations. AJR Am J Roentgenol 1989;152:765-70.

22. Rameshbabu CS, Wani ZA, Rai P, et al. Standard imaging techniques for assessment of portal venous system and its tributaries by linear endoscopic ultrasound: a pictorial essay. Endosc Ultrasound 2013;2:16-34.

23. Incedayı M, Arıbal S, Sivrioğlu AK, et al. Are hepatic portal venous system components distributed equally in the liver? A multidetector computerized tomography study. Balkan Med J 2012;29:419-23.

24. Gallix BP, Reinhold C, Dauzat M, et al. Streamlined flow in the portal vein: demonstration with MR angiography. J Magn Reson Imaging 2002;15:603-9.

25. Stankovic Z, Frydrychowicz A, Csatari Z, et al. MR-based visualization and quantification of three-dimensional flow characteristics in the portal venous system. J Magn Reson Imaging 2010;32:466-75.

26. Stankovic Z, Csatari Z, Deibert P, et al. A feasibility study to evaluate splanchnic arterial and venous hemodynamics by flow-sensitive 4D MRI compared with Doppler ultrasound in patients with cirrhosis and controls. Eur J Gastroenterol Hepatol 2013;25:669-75.

27. Orth RC, Wallace MJ, Kuo MD, et al. C-arm cone-beam CT: general principles and technical considerations for use in interventional radiology. J Vasc Interv Radiol 2008;19:814-20.

28. Casselman JW, Gieraerts K, Volders D, et al. Cone beam CT: non-dental applications. JBR-BTR 2013;96:333-53.

29. Kamran M, Nagaraja S, Byrne JV. C-arm flat detector computed tomography: the technique and its applications in interventional neuro-radiology. Neuroradiology 2010;52:319-27.

30. Iwazawa J, Ohue S, Hashimoto N, et al. Survival after C-arm CT-assisted chemoembolization of unresectable hepatocellular carcinoma. Eur J Radiol 2012;81:3985-92.

31. Louie JD, Kothary N, Kuo WT, et al. Incorporating cone-beam CT into the treatment planning for yttrium-90 radioembolization. J Vasc Interv Radiol 2009;20:606-13.

32. Kalia A, Gurajala RK, Sands MJ, et al. Venous phase C-arm cone beam CT in portomesenteric venous thrombosis: diagnostic value in assessing collateral pathways compared to digital subtraction angiogram. J Vasc Interv Radiol 2015;26:S121.

33. Siewerdsen JH, Jaffray DA. Cone-beam computed tomography with a flat-panel imager: magnitude and effects of x-ray scatter. Med Phys 2001;28:220-31.

34. Yu L, Vrieze TJ, Bruesewitz MR, et al. Dose and image quality evaluation of a dedicated cone-beam CT system for high-contrast neurologic applications. AJR Am J Roentgenol 2010;194:W193-201.

35. Shiomi S, Kuroki T, Ueda T, et al. Measurement of portal systemic shunting by oral and per-rectal administration of [123I]iodoamphetamine, and clinical use of the results. Am J Gastroenterol 1994;89:86-91.

36. Katz AI, Chen Y, Moreno AH. Flow through a collapsible tube. Experimental analysis and mathematical model. Biophys J 1969;9:1261-79.

37. Meissner MH, Moneta G, Burnand K, et al. The hemodynamics and diagnosis of venous disease. J Vasc Surg 2007;46 Suppl S:4S-24S.

38. Labropoulos N, Borge M, Pierce K, et al. Criteria for defining significant central vein stenosis with duplex ultrasound. J Vasc Surg 2007;46:101-7.

39. Zaharchuk G, Fischbein NJ, Rosenberg J, et al. Comparison of MR and contrast venography of the cervical venous system in multiple sclerosis. AJNR Am J Neuroradiol 2011;32:1482-9.

40. Horton KM, Fishman EK. Volume-rendered 3D CT of the mesenteric vasculature: normal anatomy, anatomic variants, and pathologic conditions. Radiographics 2002;22:161-72.

41. Vedantham S, Lu DS, Reber HA, et al. Small peripancreatic veins: improved assessment in pancreatic cancer patients using thin-section pancreatic phase helical CT. AJR Am J Roentgenol 1998;170:377-83.

42. Qi X, Han G. Transjugular intrahepatic portosystemic shunt in the treatment of portal vein thrombosis: a critical review of literature. Hepatol Int 2012;6:576-90.

43. Walser EM, Soloway R, Raza SA, et al. Transjugular portosystemic shunt in chronic portal vein occlusion: importance of segmental portal hypertension in cavernous transformation of the portal vein. J Vasc Interv Radiol 2006;17:373-8.

44. Spaander MC, van Buuren HR, Hansen BE, et al. Ascites in patients with noncirrhotic nonmalignant extrahepatic

cdt.amegroups.com *Cardiovasc Diagn Ther* 2016;6(6):544-556

portal vein thrombosis. Aliment Pharmacol Ther 2010;32:529-34.

45. Wong S, Cristescu M, Angle JF, et al. Diagnosis and treatment of isolated splenic vein thrombosis. J Vasc Interv Radiol 2014;25:S194-S195.

46. Hawkins CM, Kukreja K, Singewald T, et al. Use of cone-beam CT and live 3-D needle guidance to facilitate percutaneous nephrostomy and nephrolithotripsy access in children and adolescents. Pediatr Radiol 2016;46:570-4.

47. Abi-Jaoudeh N, Kobeiter H, Xu S, et al. Image fusion during vascular and nonvascular image-guided procedures. Tech Vasc Interv Radiol 2013;16:168-76.

48. Ketelsen D, Groezinger G, Maurer M, et al. Three-dimensional C-arm CT-guided transjugular intrahepatic portosystemic shunt placement: Feasibility, technical success and procedural time. Eur Radiol 2016;26:4277-83.

49. Chen GH. C-arm cone-beam CT imaging in future ischemic acute stroke treatment: one-stop-shop imaging. 57th Annual Meeting & Exhibition. Anaheim, CA, USA,

July 14, 2015.

50. Yang P, Niu K, Wu Y, et al. Time-Resolved C-Arm Computed Tomographic Angiography Derived From Computed Tomographic Perfusion Acquisition: New Capability for One-Stop-Shop Acute Ischemic Stroke Treatment in the Angiosuite. Stroke 2015;46:3383-9.

51. Kane GC, Doyle BJ, Lerman A, et al. Ultra-low contrast volumes reduce rates of contrast-induced nephropathy in patients with chronic kidney disease undergoing coronary angiography. J Am Coll Cardiol 2008;51:89-90.

52. Andò G, de Gregorio C, Morabito G, et al. Renal function-adjusted contrast volume redefines the baseline estimation of contrast-induced acute kidney injury risk in patients undergoing primary percutaneous coronary intervention. Circ Cardiovasc Interv 2014;7:465-72.

53. Kim S, Yoshizumi TT, Toncheva G, et al. Comparison of radiation doses between cone beam CT and multi detector CT: TLD measurements. Radiat Prot Dosimetry 2008;132:339-45.